MIT Open Access Articles

Reciprocity-Enhanced Optical Communication Through Atmospheric Turbulence—Part II: Communication Architectures and Performance

Reciprocity-Enhanced Optical Communication through Atmospheric Turbulence—Part II: Communication Architectures and Performance

Andrew L. Puryear[a], Jeffrey H. Shapiro[b], and Ronald R. Parenti[a]

[a]MIT Lincoln Laboratory, Lexington, Massachusetts 02139, USA
[b]Research Laboratory of Electronics, Massachusetts Institute of Technology, Cambridge, Massachusetts 02139, USA

ABSTRACT

Free-space optical communication provides rapidly deployable, dynamic communication links that are capable of very high data rates compared with those of radio-frequency systems. As such, free-space optical communication is ideal for mobile platforms, for platforms that require the additional security afforded by the narrow divergence of a laser beam, and for systems that must be deployed in a relatively short time frame. In clear-weather conditions the data rate and utility of free-space optical communication links are primarily limited by fading caused by micro-scale atmospheric temperature variations that create parts-per-million refractive-index fluctuations known as atmospheric turbulence. Typical communication techniques to overcome turbulence-induced fading, such as interleavers with sophisticated codes, lose viability as the data rate is driven higher or the delay requirement is driven lower. This paper, along with its companion [J. H. Shapiro and A. Puryear, "Reciprocity-Enhanced Optical Communication through Atmospheric Turbulence–Part I: Reciprocity Proofs and Far-Field Power Transfer"], present communication systems and techniques that exploit atmospheric reciprocity to overcome turbulence which are viable for high data rate and low delay requirement systems. Part I proves that reciprocity is exhibited under rather general conditions, and derives the optimal power-transfer phase compensation for far-field operation. The Part II paper presents capacity-achieving architectures that exploit reciprocity to overcome the complexity and delay issues that limit state-of-the art free-space optical communications. Further, this paper uses theoretical turbulence models to determine the performance—delay, throughput, and complexity—of the proposed architectures.

Keywords: optical communication, clear air turbulence, reciprocity

1. INTRODUCTION

Free-space optical (FSO) communication can help satisfy the emergent requirement to be able to detect anything, from anywhere, at any time with a requirement to globally share this information in real-time with high reliability and security. In clear-weather conditions the data rate and utility of free-space optical communication links are primarily limited by fading caused by micro-scale atmospheric temperature variations that create parts-per-million refractive-index fluctuations known as atmospheric turbulence. Typical communication techniques to overcome turbulence-induced fading, such as interleavers with sophisticated codes, lose viability as the data rate is driven higher or the delay requirement is driven lower. Using the reciprocal nature of the turbulent atmosphere, we will describe communication techniques to overcome turbulence that are viable for high data rate and low delay systems.

Reciprocity promises to be a disruptive technology for high data rate free-space optical communication through atmospheric turbulence. By exploiting reciprocity, systems can overcome the complexity and delay issues that limit state-of-the art free-space optical communications. Additionally, with the proper system design, reciprocity provides turbulence state information for free. In other words, bidirectional links, or unidirectional links employing a beacon for tracking purposes, can measure the instantaneous turbulence state without additional complexity or loss of performance. In this paper we explore the benefits of reciprocity in free-space optical communication systems. For average-power limited systems, i.e., systems in which power can be allocated across independent turbulence realizations, communication techniques that exploit reciprocity can be used to increase the ergodic capacity, decrease the decoder complexity, and reduce the system delay. For peak-power limited systems, viz., systems in which power cannot be allocated across independent turbulence realizations, the ergodic capacity cannot be increased by using reciprocity unless adaptive optics are employed. Nevertheless, when these systems do not use adaptive optics, reciprocity can be used to decrease decoder complexity and reduce system delay while still achieving ergodic capacity. The data rate of many systems, whether peak or average power limited, is limited by decoder complexity, in which case reciprocity can increase the implementable data rate. Further, if adaptive optical compensation is used, reciprocity can be used to increase the capacity of optical communication systems by increasing power-transfer efficiency. Most optical communication transmitters are peak-power limited, because of the use of components—such as Erbium-doped power amplifiers—whose time constants are much shorter than the atmospheric coherence time. Further, as signaling rates continue to increase, all transmitters become effectively peak-power limited. As a result, we focus on peak-power limited systems in this paper.

In this paper, we introduce a new performance metric that replaces ergodic capacity with something more appropriate for systems utilizing reciprocity. We use the new performance metric to calculate the optimal performance for systems utilizing perfect and imperfect reciprocity. We determine the performance of architectures that are optimal and architectures that are particularly amenable to implementation. Reciprocity can be used to inform adaptive optics (AO) compensation,[1] but, although our results apply to both AO compensated and uncompensated systems, we do not explicitly address the performance improvement afforded by adaptive optics compensation. Instead we focus on coding, interleaving, and power control to improve performance.

2. CHANNEL MODELS

We consider a line-of-sight, single spatial-mode system—either for bidirectional communication or unidirectional communication with a return-path tracking beacon—whose $z = 0$ plane transceiver has an exit/entrance pupil $\mathcal{A}_0$ of area A_0, and whose $z = L$ plane transceiver has an exit/entrance pupil $\mathcal{A}_L$ of area A_L. Data is transmitted from the $z = 0$ plane transmitter and received coherently or incoherently by the data receiver in the $z = L$ plane. In the reverse direction, a data stream or a beacon is transmitted from the $z = L$ plane and received coherently or incoherently in the $z = 0$ plane. Each transceiver employs a diplexer that enables it to use fiber-coupled lasers and photodetectors in distinct focal planes that share the terminal's common exit/entrance pupil.

We assume linear-polarized operation at center frequency ω_0 (center wavelength $\lambda = 2\pi c/\omega_0$), and use the following scalar baseband model for the complex field envelope in the $z = 0$ to $z = L$ link's receiver fiber at time t:

$$s_{L_R}(t) = \sqrt{\alpha_{0L}(t)}\nu_{0L}(t)s_{0_T}(t - L/c) + w_{L_R}(t). \tag{1}$$

Here: $s_{0_T}(t)$ is the scalar complex envelope of the field transmitted from the $z = 0$ plane at time t, which satisfies $|s_{0_T}(t)|^2 \leq P_{0_T}$ for a peak-power limited system; $\nu_{0L}(t)$ represents the turbulence-induced amplitude and phase fluctuations imposed on a field transmitted from $z = 0$ at time $t - L/c$ and received at $z = L$ at time t, which is normalized to satisfy $\mathbb{E}[|\nu_{0_L}(t)|^2] = 1$, so that $\alpha_{0_L}(t)$ is the average $z = 0$ to $z = L$ power-transfer efficiency at time t; and $w_{L_R}(t)$ is the complex field envelope of the background light entering the $z = L$ plane receiver's fiber at time t.

From the extended Huygens-Fresnel principle[2,3] we have that the average $z = 0$ to $z = L$ power-transfer efficiency at time t is

$$\alpha_{0L}(t) = \mathbb{E}\left[\left|\int_{\mathcal{A}_0}\int_{\mathcal{A}_L} p_{0_T}(\boldsymbol{\rho})T_{0_T}(\boldsymbol{\rho};t-L/c)h(\boldsymbol{\rho}',\boldsymbol{\rho};t)T_{L_R}(\boldsymbol{\rho}';t)p_{L_R}(\boldsymbol{\rho}')d\boldsymbol{\rho}'d\boldsymbol{\rho}\right|^2\right], \tag{2}$$

where: $h(\boldsymbol{\rho}',\boldsymbol{\rho};t)$, for $\boldsymbol{\rho} \in \mathcal{A}_0$ and $\boldsymbol{\rho}' \in \mathcal{A}_\mathcal{L}$, is the atmospheric propagation Green's function at time t; $p_{0_T}(\boldsymbol{\rho})$ is the mode function produced by the $z = 0$ transmitter's fiber in the $\mathcal{A}_0$ exit pupil; $p_{L_R}(\boldsymbol{\rho}')$ is the mode function that couples light from the $z = L$ receiver's $\mathcal{A}_L$ entrance pupil to its receiver fiber; $T_{0_T}(\boldsymbol{\rho};t)$ is the $z = 0$ transmitter's AO transformation at time t; and $T_{L_R}(\boldsymbol{\rho}';t)$ is the $z = L$ receiver's AO transformation at time t. If adaptive optics are not used, these AO transformations are $T_{0_T}(\boldsymbol{\rho};t) = 1$ and $T_{L_R}(\boldsymbol{\rho}';t) = 1$. If phase-only adaptive optics are used, then $T_{0_T}(\boldsymbol{\rho};t) = e^{-j\theta_{0_T}(\boldsymbol{\rho};t)}$ and $T_{L_R}(\boldsymbol{\rho}';t) = e^{-j\theta_{L_R}(\boldsymbol{\rho}';t)}$. The normalized turbulence state for the field propagating from the $z = 0$ to the $z = L$ plane is given by,

$$\nu_{0L}(t) = \frac{\int_{\mathcal{A}_0}\int_{\mathcal{A}_L} p_{0_T}(\boldsymbol{\rho})T_{0_T}(\boldsymbol{\rho};t-L/c)h(\boldsymbol{\rho}',\boldsymbol{\rho};t)T_{L_R}(\boldsymbol{\rho}';t)p_{L_R}(\boldsymbol{\rho}')d\boldsymbol{\rho}'d\boldsymbol{\rho}}{\sqrt{\alpha_{0L}(t)}}. \tag{3}$$

The background-light contribution to $s_{L_r}(t)$ is a zero-mean, circulo-complex Gaussian random process whose mean-squared strength is

$$\mathbb{E}[|w_{L_R}(t)|^2] = \lambda^2 N_{L_\lambda}\Delta\lambda_L, \tag{4}$$

where N_{L_λ} is the background-light spectral radiance at the $z = L$ plane and $\Delta\lambda_L$ is the wavelength-units bandwidth of the background-suppressing optical filter employed in the $z = L$ plane's receiver. The preceding results imply that the $z = L$ receiver's photon detection rate at time t is

$$\mu_{L_R}(t) = \frac{\eta_L\left|\sqrt{\alpha_{0L}(t)}\nu_{0L}(t)s_{0_T}(t-L/c) + w_{L_R}(t)\right|^2}{\hbar\omega_0}, \tag{5}$$

where η_L is its detector's quantum efficiency.

Our model for the $z = L$ to $z = 0$ channel parallels the development we have just completed for $z = 0$ to $z = L$ propagation. The scalar complex envelope of the field entering the $z = 0$ receiver's fiber at time t is

$$s_{0_R}(t) = \sqrt{\alpha_{L0}(t)}\nu_{L0}(t)s_{L_T}(t-L/c) + w_{0_R}(t), \tag{6}$$

where $s_{L_T}(t)$ is the complex envelope of the field transmitted from the $z = L$ plane, $\nu_{L0}(t)$ is the normalized turbulence state for a field transmitted from $z = L$ at time $t - L/c$ and received at $z = 0$ at time t, $\alpha_{L0}(t)$ is the average $z = L$ to $z = 0$ power-transfer efficiency at time t, and $w_{0_R}(t)$ is the complex envelope of the background light entering the $z = 0$ receiver's fiber at time t. For peak-power limited systems $|s_{L_T}(t)|^2 \leq P_{L_T}$.

Using extended Huygens-Fresnel principle, and the reciprocity of its Green's function,[4] the average $z = L$ to $z = 0$ power-transfer efficiency at time t is,

$$\alpha_{L0}(t) = \mathbb{E}\left[\left|\int_{\mathcal{A}_0}\int_{\mathcal{A}_L} p_{0_R}(\boldsymbol{\rho})T_{0_R}(\boldsymbol{\rho};t)h(\boldsymbol{\rho}',\boldsymbol{\rho};t)T_{L_T}(\boldsymbol{\rho}';t-L/c)p_{L_T}(\boldsymbol{\rho}')d\boldsymbol{\rho}'d\boldsymbol{\rho}\right|^2\right], \tag{7}$$

where: $p_{L_T}(\boldsymbol{\rho}')$ is the mode function produced by the $z = L$ transmitter's fiber in the $\mathcal{A}_L$ exit pupil; $p_{0_R}(\boldsymbol{\rho})$ is the mode function that couples light from $z = 0$ receiver's $\mathcal{A}_0$ entrance pupil to its receiver fiber; $T_{L_T}(\boldsymbol{\rho}';t)$ is the $z = L$ transmitter's AO transformation at time t; and $T_{0_R}(\boldsymbol{\rho}';t)$ is the $z = 0$ receiver's AO transformation

at time t.. The normalized turbulence state for the field propagating from the $z = L$ to the $z = 0$ plane is given by,

$$\nu_{L0}(t) = \frac{\underset{\mathcal{A}_0}{\int}\underset{\mathcal{A}_L}{\int} p_{0_R}(\boldsymbol{\rho})T_{0_R}(\boldsymbol{\rho};t)h(\boldsymbol{\rho}',\boldsymbol{\rho};t)T_{L_T}(\boldsymbol{\rho}';t-L/c)p_{L_T}(\boldsymbol{\rho}')d\boldsymbol{\rho}'d\boldsymbol{\rho}}{\sqrt{\alpha_{L0}(t)}}, \tag{8}$$

The background-light contribution to $s_{0_r}(t)$ is a zero-mean, circulo-complex Gaussian random process whose mean-squared strength is

$$\mathbb{E}[|w_{0_R}(t)|^2] = \lambda^2 N_{0_\lambda}\Delta\lambda_0, \tag{9}$$

where N_{0_λ} is the background-light spectral radiance at the $z = 0$ plane and $\Delta\lambda_0$ is the wavelength-units bandwidth of the background-suppressing optical filter employed in the $z = 0$ plane's receiver. The $z = 0$ receiver's photon detection rate at time t is therefore

$$\mu_{0_R}(t) = \frac{\eta_0 \left| \sqrt{\alpha_{L0}(t)}\nu_{L0}(t)s_{L_T}(t-L/c) + w_{0_R}(t) \right|^2}{\hbar\omega_0}, \tag{10}$$

where η_0 is its detector's quantum efficiency.

The $z = 0$ to $z = L$ and $z = L$ to $z = 0$ channel models we have just specified are sufficiently general to describe fading effects on a wide range of single-mode systems by choice of the mode functions $\{p_{0_T}(\boldsymbol{\rho}), p_{0_R}(\boldsymbol{\rho}), p_{L_T}(\boldsymbol{\rho}'), p_{L_R}(\boldsymbol{\rho}')\}$, and the possibly time-varying AO transformations $\{T_{0_T}(\boldsymbol{\rho};t), T_{0_R}(\boldsymbol{\rho};t), T_{L_T}(\boldsymbol{\rho}';t), T_{L_R}(\boldsymbol{\rho}';t)\}$. For example, this model captures the behavior of the single-mode-fiber coupled system, with coherent or incoherent detection, shown in Fig. 1, which has been shown to exhibit perfect reciprocity,[5] i.e.,

$$\begin{aligned} \nu(t) &\equiv \nu_{L0}(t) = \nu_{0L}(t) \\ \alpha(t) &\equiv \alpha_{L0}(t) = \alpha_{0L}(t). \end{aligned} \tag{11}$$

These results followed from assuming that all the fibers in Fig. 1 had the same spatial mode $\xi(\cdot)$, and that single AO elements were used for both the transmitter and the receiver at $z = 0$ and $z = L$. The first assumption implies that

$$\begin{aligned} p_0(\boldsymbol{\rho}) &\equiv p_{0_T}(\boldsymbol{\rho}) = p_{0_R}(\boldsymbol{\rho}) = \int_{\mathcal{F}_0} \xi(\boldsymbol{\rho}_f)g_0(\boldsymbol{\rho},\boldsymbol{\rho}_f)d\boldsymbol{\rho}_f \\ p_L(\boldsymbol{\rho}') &\equiv p_{L_T}(\boldsymbol{\rho}') = p_{L_R}(\boldsymbol{\rho}') = \int_{\mathcal{F}_L} \xi(\boldsymbol{\rho}'_f)g_L(\boldsymbol{\rho}',\boldsymbol{\rho}'_f)d\boldsymbol{\rho}'_f, \end{aligned} \tag{12}$$

where $\boldsymbol{\rho}_f \in \mathcal{F}_0$ is a vector in the exit facet of the $z = 0$ fiber, $\boldsymbol{\rho}'_f \in \mathcal{F}_L$ is a vector in the exit facet of the $z = L$ fiber, $g_0(\boldsymbol{\rho},\boldsymbol{\rho}_f)$ is the response at $\boldsymbol{\rho} \in \mathcal{A}_0$ to an impulse (point source) at $\boldsymbol{\rho}_f \in \mathcal{F}_0$, and $g_L(\boldsymbol{\rho},\boldsymbol{\rho}_f)$ is the response at $\boldsymbol{\rho}' \in \mathcal{A}_L$ to an impulse (point source) at $\boldsymbol{\rho}'_f \in \mathcal{F}_L$. The second assumption implies that $T_0(\boldsymbol{\rho};t) \equiv T_{0_T}(\boldsymbol{\rho};t) = T_{0_R}(\boldsymbol{\rho};t)$ and $T_L(\boldsymbol{\rho}';t) \equiv T_{L_T}(\boldsymbol{\rho}';t) = T_{L_R}(\boldsymbol{\rho}';t)$. Substituting $p_0(\boldsymbol{\rho})$, $p_L(\boldsymbol{\rho}')$, $T_0(\boldsymbol{\rho};t)$, and $T_L(\boldsymbol{\rho}';t)$ into our expressions for $\alpha_{0L}(t)$, $\alpha_{L0}(t)$, $\nu_{0L}(t)$, and $\nu_{L0}(t)$ yields the reciprocity relations given above.

Figure 2 shows another example encompassed by our channel models. Here we continue to assume that single AO elements are used for both the the transmitter and receiver at $z = 0$ and $z = L$, but now the transmitter and receiver at each terminal use fibers with different spatial modes, i.e.,

$$\begin{aligned} p_{0_T}(\boldsymbol{\rho}) &= \int_{\mathcal{F}_0} \xi_{0_T}(\boldsymbol{\rho}_f)g_0(\boldsymbol{\rho},\boldsymbol{\rho}_f)d\boldsymbol{\rho}_f \\ p_{0_R}(\boldsymbol{\rho}) &= \int_{\mathcal{F}_0} \xi_{0_R}(\boldsymbol{\rho}_f)g_0(\boldsymbol{\rho},\boldsymbol{\rho}_f)d\boldsymbol{\rho}_f \\ p_{L_T}(\boldsymbol{\rho}') &= \int_{\mathcal{F}_L} \xi_{L_T}(\boldsymbol{\rho}'_f)g_L(\boldsymbol{\rho}',\boldsymbol{\rho}'_f)d\boldsymbol{\rho}'_f \\ p_{L_R}(\boldsymbol{\rho}') &= \int_{\mathcal{F}_L} \xi_{L_R}(\boldsymbol{\rho}'_f)g_L(\boldsymbol{\rho}',\boldsymbol{\rho}'_f)d\boldsymbol{\rho}'_f. \end{aligned} \tag{13}$$
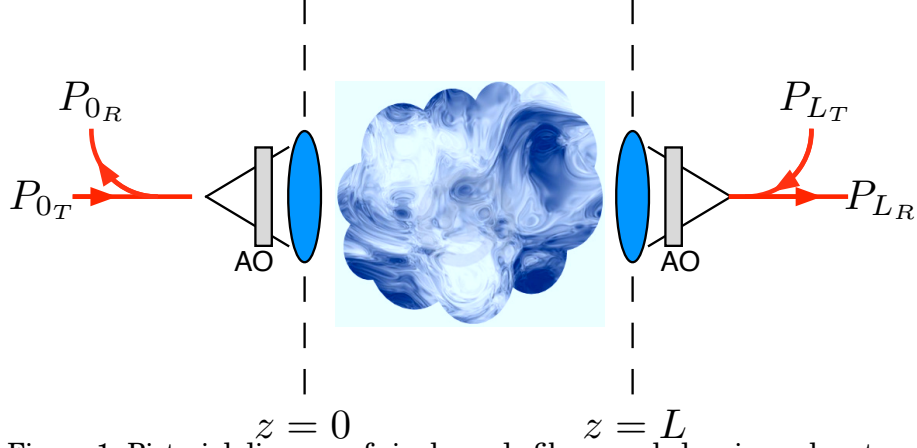
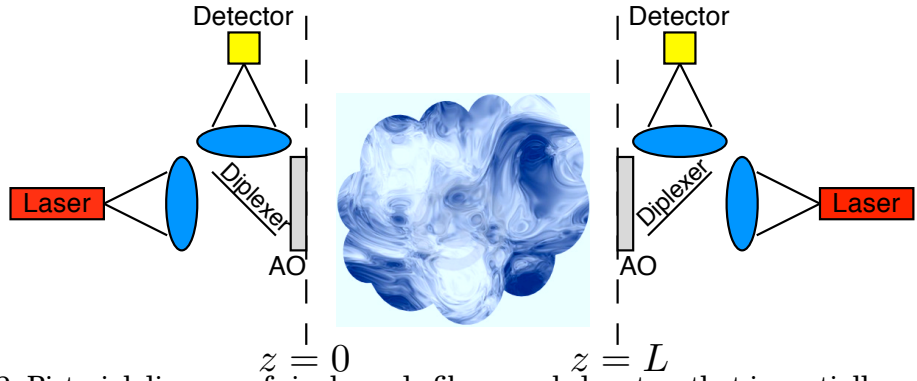Figure 1: Pictorial diagram of single mode fiber-coupled reciprocal system.

Figure 2: Pictorial diagram of single mode fiber-coupled system that is partially reciprocal.

This system does not exhibit perfect reciprocity and, as a result, $\nu_{L0}(t) \neq \nu_{0L}(t)$ and $\alpha_{L0}(t) \neq \alpha_{0L}(t)$. Nevertheless, the correlation between $\nu_{L0}(t)$ and $\nu_{0L}(t)$ may be sufficiently high, depending on the fiber-facet modes that are used, that the resulting partial reciprocity could be exploited to good effect. Thus in what follows we will consider both perfect and partial reciprocal systems in our performance analyses.

3. PERFORMANCE METRIC

The limit on reliable communication over a fading channel is often taken to be the maximum system throughput without regard for delay or system complexity. This measure is the ergodic channel capacity, viz., the channel capacity averaged over all channel state realizations. The canonical ergodic capacity for our $z = 0$ to $z = L$ link through atmospheric turbulence is thus

$$C_{0L}^{\text{ergodic}} = \mathbb{E}\left[C\left(|\nu_{0L}|^2; \Upsilon_{0_T}\left(|\nu_{0L}|^2\right), \Upsilon_{L_R}\left(|\nu_{0L}|^2\right)\right)\right]. \tag{14}$$

In this expression, $C\left(\gamma; \Upsilon_{0_T}(\gamma), \Upsilon_{L_R}(\gamma)\right)$ is the channel capacity of a particular $z = 0$ to $z = L$ turbulence state, γ, when the $z = 0$ transmitter has knowledge $\Upsilon_{0_T}(\gamma)$ of the $z = 0$ to $z = L$ turbulence state and the $z = L$ receiver has knowledge $\Upsilon_{L_R}(\gamma)$ of the $z = 0$ to $z = L$ turbulence state. If the system is peak-power limited, then the transmit power for the ergodic capacity calculation is not allowed to vary with the turbulence state. Conversely, if the system is average-power limited, then the transmit power for the ergodic capacity calculation is allowed to vary with the turbulence state. Depending on the observation of the channel state, the receiver may have no knowledge of the channel state, $\Upsilon_{L_R}(|\nu_{0L}|^2) = \emptyset$, perfect knowledge of the channel state, $\Upsilon_{L_R}(|\nu_{0L}|^2) = |\nu_{0L}|^2$, knowledge of the channel state's probability density, $\Upsilon_{L_R}(|\nu_{0L}|^2) = p_{|\nu_{0L}|^2}(\cdot)$, and similarly for the transmitter's state knowledge. Note that here and in what follows we are assuming that the turbulence-induced phase fluctuations of the single-mode received

field—which are of significance for coherent detection—are being accurately tracked, so that it only the normalized power transfer, $|\nu_{0L}|^2$, that is of interest with regards to exploiting reciprocity.

The canonical ergodic capacity is applicable to fast-fading channels, in which the latency requirement is greater than the coherence time and the codeword length spans many coherence periods. As a result, this metric is appropriate for average-power and peak-power limited systems that do not have a latency requirement. For slow-fading channels, in which the latency requirement is smaller than the coherence time and the codeword length cannot span many coherence periods, another performance metric is needed. In the slow-fading regime, performance is often measured by the maximum throughput that can be guaranteed with some probability. This measure is the ε-capacity metric given by

$$\varepsilon_{0L} = \Pr\left(C\left(|\nu_{0L}|^2; \Upsilon_{0_T}\left(|\nu_{0L}|^2\right), \Upsilon_{L_R}\left(|\nu_{0L}|^2\right)\right) < R_{0L}^{\varepsilon}\right), \tag{15}$$

so that R_{0L}^{ε} is the maximum throughput for the $z = 0$ to $z = L$ link that can be guaranteed with probability $1 - \varepsilon_{0L}$. The ε-capacity metric recognizes that, because of the stochastic nature of turbulence-induced fading, outages will occur with some probability. This metric, however, fails to account for the fact that a system can achieve ε-capacity without maximizing throughput when advantageous channel states occur. To overcome this deficiency, we define a low-delay ergodic capacity as the maximum average capacity when the system is required to meet a latency constraint, namely the time it takes for a single codeword to traverse the channel,

$$R_{0L}^{\mathrm{LD}}(\varepsilon_{0L}) = \mathbb{E}\left[\max_{d < t_0} C_{\varepsilon_{0L}}\left(|\nu_{0L}|^2; \Upsilon_{0_T}\left(|\nu_{0L}|^2\right), \Upsilon_{L_R}\left(|\nu_{0L}|^2\right)\right)\right], \tag{16}$$

where the d is the latency and t_0 is the turbulence coherence time. The ε_{0L} argument is employed because—with the channel state perhaps imperfectly known to the transmitter, and the delay required to be smaller than a coherence time—there is some probability, ε_{0L}, that data will be lost. Thus ε_{0L} is an outage probability, but it is different from the outage probability in the ε-capacity. Because of the latency requirement, the low-delay ergodic capacity is the average capacity when the system is required to maximize throughput *of each channel realization*. We will see that its outage probability can be made arbitrarily small, but only at the expense of decreasing throughput. The low-delay ergodic capacity is a generalization of canonical ergodic capacity in the sense that if the transmitter and receiver have *perfect* knowledge of the instantaneous channel state, then the low-delay ergodic capacity simplifies to the canonical ergodic capacity. It is also in this sense that low-delay ergodic capacity is a good metric for the value of reciprocity: with perfect channel reciprocity and noiseless channel measurements the low-delay ergodic capacity equals the canonical ergodic capacity. As reciprocity is degraded, the low-delay ergodic capacity of the system is strictly less than the canonical ergodic capacity. We define the power margin

$$m_{0L}\left(\varepsilon_{0L}\right) = \arg_{\beta}\left\{\mathbb{E}\left[\max_{d < t_0} C_{\varepsilon_{0L}}\left(\sqrt{\beta}|\nu_{0L}|^2; \Upsilon_{0_T}(|\nu_{0L}|^2), \Upsilon_{L_R}(|\nu_{0L}|^2)\right)\right] = \mathbb{E}\left[C\left(|\nu_{0L}|^2; |\nu_{0L}|^2, |\nu_{0L}|^2\right)\right]\right\}, \tag{17}$$

as a means to compare systems that require low delay to systems without a delay requirement. In one sense, this quantity represents the extra power required to meet the delay requirement and reduce the decoder complexity. In another sense, it is the power penalty incurred by imperfect—due to a noisy measurement or imperfect reciprocity—turbulence-state knowledge.

4. RECIPROCITY ARCHITECTURES

In theory, a configuration with perfect reciprocity can provide noiseless turbulence-state information to the transmitter, but in practice a noiseless measurement is impossible. Thus, owing to finite signal-to-noise ratio in the channel-measurement subsystem, any transmitter utilizing the reciprocity information must be robust to uncertainty in turbulence-state knowledge. Further, some hardware designs, such as those that do not couple into single-mode fiber, will only exhibit partial reciprocity, i.e., the correlation coefficient between $|\nu_{0L}|^2$ and $|\nu_{L0}|^2$ will be less than one in magnitude. These systems can also realize performance gains from the turbulence-state knowledge provided by their partial reciprocity, but they too

must be robust to uncertainty in the state measurement. In this section we present two architectures that exploit reciprocity in a robust manner. The first uses the information provided by reciprocity in an optimal manner to achieve the low-delay ergodic capacity. The second uses the information provided by reciprocity in a simple to implement manner that does not achieve the low-delay ergodic capacity.

We will use $y_{0_T}\left(\Upsilon_{0_T}\left(|\nu_{0L}|^2\right)\right)$ to denote the $z = 0$ terminal's estimate of the $z = 0$ to $z = L$ channel state, $|\nu_{0L}|^2$, based on its noisy observation of the channel state, $|\nu_{L0}|^2$, governing the light it receives from the $z = L$ transmitter. The low-delay ergoditic capacity for $z = 0$ to $z = L$ channel is then

$$
\begin{aligned}
R_{0L}^{\mathrm{LD}}(\varepsilon_{0L}) &= \mathbb{E}\left[\max_{d<t_0} C_{\varepsilon_{0L}}\left(|\nu_{0L}|^2; \Upsilon_{0_T}\left(|\nu_{0L}|^2\right), \Upsilon_{L_R}\left(|\nu_{0L}|^2\right)\right)\right] \\
&= \max_{y_{0_T}(\cdot):\mathrm{Pr}\left(y_{0_T}(\gamma)>|\nu_{0L}|^2\middle|\Upsilon_{0_T}(|\nu_{0L}|^2)=\gamma\right)<\varepsilon_{0L}\forall\gamma} \\
&\qquad \int C\left(y_{0_T}(\gamma)\right)\mathrm{Pr}\left(y_{0_T}(\gamma) < |\nu_{0L}|^2\middle|\Upsilon_{0_T}(|\nu_{0L}|^2) = \gamma\right) f_{\Upsilon_{0_T}(|\nu_{0L}|^2)}(\gamma)d\gamma \\
&= \max_{y_{0_T}(\cdot):F_{|\nu_{0L}|^2|\Upsilon_{0_T}(|\nu_{0L}|^2)}(y_{0_T}(\gamma))<\varepsilon_{0L}\forall\gamma} \int C(y_{0_T}(\gamma))\left(1 - F_{|\nu_{0L}|^2|\Upsilon_{0_T}(|\nu_{0L}|^2)}(y_{0_T}(\gamma))\right) f_{\Upsilon_{0_T}(|\nu_{0L}|^2)}(\gamma)d\gamma \\
&= \max_{y_{0_T}(\cdot):F_{|\nu_{0L}|^2|\Upsilon_{0_T}(|\nu_{0L}|^2)}(y_{0_T}(\gamma))<\varepsilon_{0L}\forall\gamma} (1 - \varepsilon_{0L})\int C(y_{0_T}(\gamma))f_{\Upsilon_{0_T}(|\nu_{0L}|^2)}(\gamma)d\gamma,
\end{aligned}
\tag{18}
$$

where $C(y_{0_T}(\gamma))$ is the capacity of the data channel with $y_{0_T}(\gamma)$ channel gain, F_x and f_x are the cumulative distribution function and probability density function of the random variable x, respectively. Thus, the problem of maximizing low-delay ergodic capacity is reduced to finding the channel-state estimator $y_{0_T}(\cdot)$ that maximizes the capacity while guaranteeing that the channel will be in outage with probability less than ε_{0L}. Equation (18) is a general form for the low-delay ergodic capacity—it is valid for either coherent or incoherent detection and for background and signal shot-noise limited systems.

4.1 Optimal Reciprocity Architecture

From Eq. (18) it is clear that an optimal, low-delay capacity achieving, architecture is a bank of encoders and decoders, where the appropriate encoder-decoder pair is selected based on the optimal estimate of the current channel state, $y_{0_T}\left(\Upsilon_{0_T}\left(|\nu_{0L}|^2\right)\right)$. This is shown pictorially in Fig. 3.

Note that each encoder-decoder pair can be implemented with simple additive white-Gaussian noise (AWGN) channel codes. Herein lies one advantage of systems exploiting reciprocity—systems exploiting reciprocity simply use a bank of AWGN codes. This is in contrast to the computationally-intensive sophisticated fading-channel codes required to achieve capacity for systems without reciprocity information.

For the architecture shown in Fig. 3 to approach the low-delay ergodic capacity, the number of encoder-decoder pairs must approach infinity. For realistic implementations of this architecture, using a finite number of encoder-decoder pairs, some performance penalty will be incurred. Thus, there is a trade between the number of encoder-decoder pairs implemented and the degree to which the low-delay ergodic capacity is approached. Taking this trade to the extreme, in which there is only one encoder-decoder pair, we arrive at an architecture with greatly reduced implementation complexity that was first suggested by Greco.[6] This leads us to the *reduced implementation-complexity reciprocity architecture* in the next subsection.

4.2 Reduced Implementation-Complexity Reciprocity Architecture

The reduced implementation-complexity reciprocity architecture is just the optimal architecture taken to have only one encoder-decoder pair. It transmits at some fixed rate when the channel state is good, i.e., $|\nu_{0L}|^2$ is deemed to be sufficiently high, and does not transmit otherwise, i.e., when the channel state is bad. Thus, finding the optimal single encoder-decoder estimator reduces to simply determining, under uncertainty in channel-state knowledge, when and at what data rate to turn on the transmitter given the
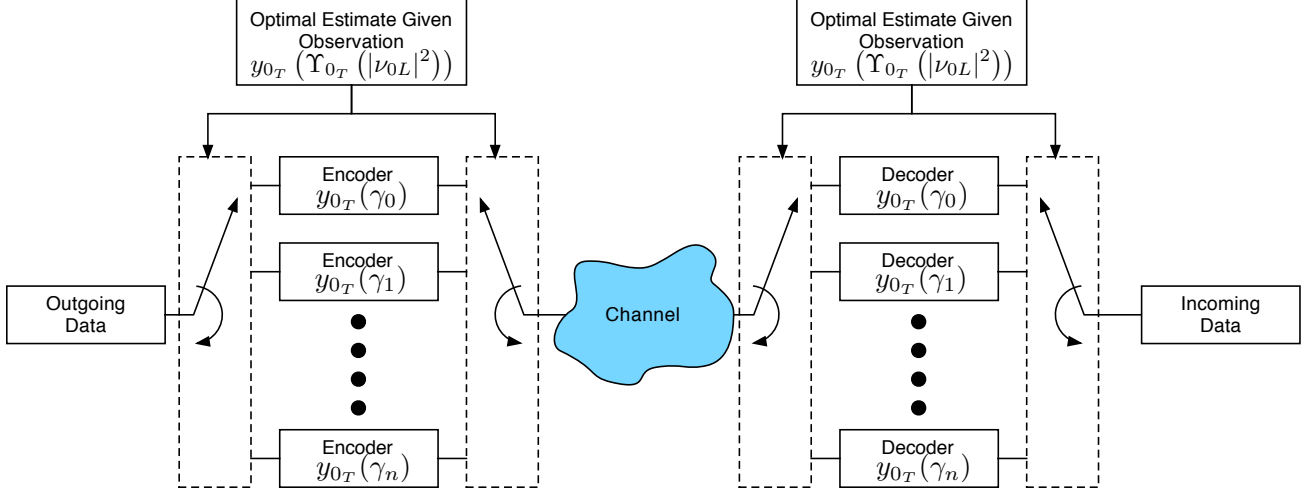
Figure 3: Pictorial diagram of the optimal reciprocity architecture for peak-power limited systems. The encoder/decoder pairs are selected based on the optimal estimate of the turbulence state given the observation of the $z = L$ to $z = 0$ channel. The encoder/decoder pairs can implement additive white-Gaussian noise (AWGN) channel codes and still retain low-delay ergodic capacity achieving performance.

throughput and outage constraints. Mathematically, this single encoder-decoder pair assumption forces the estimator to be of the form,

$$
y_{0_T}^{\text{s}} \left(\Upsilon_{0_T} \left(|\nu_{0L}|^2 \right) \right) = \begin{cases} y_{0_T}^{\text{s},0}, & \Upsilon_{0_T} \left(|\nu_{0L}|^2 \right) \geq \gamma_0 \\ 0, & \Upsilon_{0_T} \left(|\nu_{0L}|^2 \right) < \gamma_0 \end{cases}, \tag{19}
$$

where γ_0 is the threshold above which the transmitter is turned on. Thus, the optimization problem is reduced from determining a continuous, real-valued function for the optimal case to determining two real-valued parameters for the reduced-complexity case. The optimization is given by,

$$
\begin{aligned}
R_{0L}^{\text{LD,s}}(\varepsilon_{0L}) &= \max_{y_{0_T}^{\text{s},0}, \gamma_0 : F_{|\nu_{0L}|^2 | \Upsilon_{0_T}(|\nu_{0L}|^2)}(y_{0_T}^{\text{s}}(\gamma)) < \varepsilon_{0L} \forall \gamma} (1 - \varepsilon_{0L}) \int C(y_{0_T}^{\text{s}}(\gamma)) f_{\Upsilon_{0_T}(|\nu_{0L}|^2)}(\gamma) d\gamma \\
&= \max_{y_{0_T}^{\text{s},0}, \gamma_0 : F_{|\nu_{0L}|^2 | \Upsilon_{0_T}(|\nu_{0L}|^2)}(y_{0_T}^{\text{s}}(\gamma)) < \varepsilon_{0L} \forall \gamma} (1 - \varepsilon_{0L}) C \left(y_{0_T}^{\text{s},0} \right) \left(1 - F_{\Upsilon_{0_T}(|\nu_{0L}|^2)}(\gamma_0) \right),
\end{aligned} \tag{20}
$$

where $C(y_{0_T}^{\text{s},0})$ is the transmission rate when the transmitter is on, and $R_{0L}^{\text{LD,s}}(\varepsilon_{0L})$ is the low-delay ergodic capacity restricted to a single encoder-decoder pair implementation. This architecture is shown pictorially in Fig. 4. In the next section, we calculate the theoretical performance of both the optimal and and reduced-complexity architectures for various example scenarios.

5. THEORETICAL PERFORMANCE FOR PEAK-POWER LIMITED SYSTEMS

We now provide three example calculations for peak-power limited systems: (1) we show that with perfect turbulence-state knowledge at both the transmitter and receiver, the low-delay ergodic capacity is equal to the canonical ergodic capacity; (2) we show that with only statistical turbulence-state knowledge at the transmitter and perfect turbulence-state knowledge at the receiver, the low-delay ergodic capacity is equivalent to ε-capacity; and (3) we find the capacity for a system in which the turbulence state is measured by an incoherent beacon receiver and the data is received with a coherent detector. In addition to calculating the low-delay ergodic capacity, we also calculate the capacity-achieving estimator $y_{0_T}(\cdot)$ and the single encoder-decoder estimator $y_{0_T}^{\text{s}}(\cdot)$.
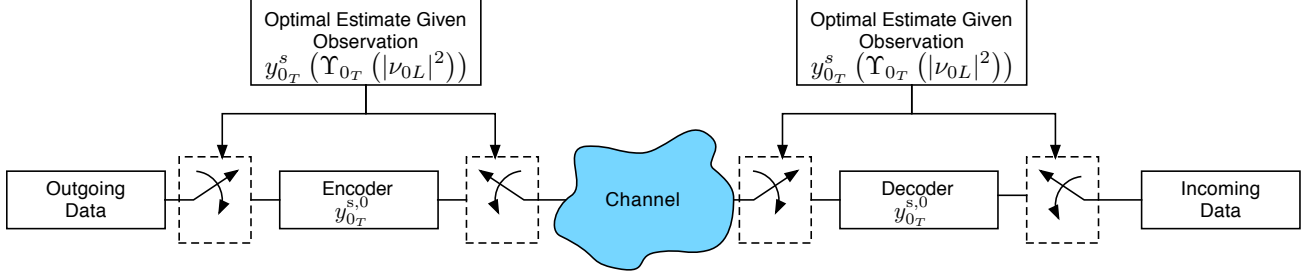
Figure 4: Pictorial diagram of the reduced implementation-complexity reciprocity architecture. In the figure, the encoder/decoder pair is selected to optimize performance when data is transmitted at rate $C(y_{0_T}^{\text{s},0})$ when $\Upsilon_{0_T}\left(|\nu_{0L}|^2\right) \geq \gamma_0$ and no data is transmitted when $\Upsilon_{0_T}\left(|\nu_{0L}|^2\right) < \gamma_0$. The encoder/decoder pair can implement an additive white-Gaussian noise (AWGN) channel code.

5.1 Perfect Turbulence-State Knowledge

For this example, we assume that the data transmitter has perfect knowledge of the instantaneous turbulence state, $\Upsilon_{0_T}\left(|\nu_{0L}|^2\right) = |\nu_{0L}|^2$. The low-delay ergodic capacity is then,

$$
\begin{aligned}
R_{0L}^{\text{LD}}(\varepsilon_{0L}) &= \max_{y_{0_T}(\cdot):F_{|\nu_{0L}|^2|\Upsilon_{0_T}(|\nu_{0L}|^2)}(y_{0_T}(\gamma))<\varepsilon_{0L}\forall\gamma} (1-\varepsilon_{0L}) \int C(y_{0_T}(\gamma)) f_{\Upsilon_{0_T}(|\nu_{0L}|^2)}(\gamma)d\gamma \\
&= \begin{cases} 0, & y_{0_T}(|\nu_{0L}|^2) > |\nu_{0L}|^2 \\ \int C(y_{0_T}(\gamma)) f_{|\nu_{0L}|^2}(\gamma)d\gamma, & y_{0_T}(|\nu_{0L}|^2) \leq |\nu_{0L}|^2 \end{cases},
\end{aligned}
\tag{21}
$$

where we have used the fact that $F_{|\nu_{0L}|^2|\Upsilon_{0_T}(|\nu_{0L}|^2)}(y_{0_T}(\gamma))$ is a step function and that $|\nu_{0L}|^2$ is a sufficient statistic for the system performance calculation. Noting that $C(\cdot)$ is a monotonically increasing function, the optimal estimator is $y_{0_T}\left(\Upsilon_{0_T}\left(|\nu_{0L}|^2\right)\right) = |\nu_{0L}|^2$. Using the optimal estimator, the low-delay ergodic capacity is,

$$
\begin{aligned}
R_{0L}^{\text{LD}}(\varepsilon_{0L}) &= \int C(\gamma) f_{|\nu_{0L}|^2}(\gamma)d\gamma \\
&= C_{0L}^{\text{ergodic}}.
\end{aligned}
\tag{22}
$$

Thus, with perfect turbulence-state knowledge, the low-delay constraint imposed in the definition of the low-delay ergodic capacity does not reduce the capacity from the unbounded delay capacity. Consequently, no extra power is required to meet the delay requirement, $m_{0L}\left(\epsilon_{0L}\right) = 0\,\text{dB}\ \forall\epsilon_{0L}$.

Because the turbulence state is known perfectly, the estimator for the single encoder-decoder architecture is simply $y_{0_T}^{\text{s}} = C(\gamma_0)$ where γ_0 is chosen to maximize the low-delay ergodic capacity,

$$
R_{0L}^{\text{LD,s}}(\varepsilon_{0L}) = \max_{\gamma_0} C(\gamma_0)\left(1 - F_{|\nu_{0L}|^2}(\gamma_0)\right),
\tag{23}
$$

where the optimization is convex with respect to γ_0. So, if γ_0 is too small, the system transmits a large proportion of the time but at a very low rate. Conversely, if γ_0 is too large, the system transmits at a very high rate, but only a small proportion of the time.

5.2 Statistical Turbulence-State Knowledge

For this example, we assume that the data transmitter only has knowledge of the statistical distribution of the turbulence state, $\Upsilon_{0_T}\left(|\nu_{0L}|^2\right) = p_{|\nu_{0L}|^2}(\cdot)$. We note that, because the turbulence-state information is independent of the actual turbulence state, the conditional cumulative distribution function is equal

to the unconditional cumulative distribution function, $F_{|\nu_{0L}|^2|\Upsilon_{0_T}(|\nu_{0L}|^2)}(\cdot) = F_{|\nu_{0L}|^2}(\cdot)$. Thus the optimal estimator is $y_{0_T} = F_{|\nu_{0L}|^2}^{-1}(\varepsilon_{0L})$ where $F_{|\nu_{0L}|^2}^{-1}(\cdot)$ is the generalized inverse distribution function, defined as

$$F_{|\nu_{0L}|^2}^{-1}(y) = \inf_{x \in \mathbb{R}} \left\{ F_{|\nu_{0L}|^2}^{-1}(x) \geq y \right\}. \tag{24}$$

Using the optimal estimator, we find the low-delay ergodic capacity with only statistical turbulence-state knowledge at the data transmitter to be,

$$
\begin{aligned}
R_{0L}^{\text{LD}}(\varepsilon_{0L}) &= \max_{y_{0_T}(\cdot):F_{|\nu_{0L}|^2|\Upsilon_{0_T}(|\nu_{0L}|^2)}(y_{0_T}(\gamma))<\varepsilon_{0L}\forall\gamma} (1-\varepsilon_{0L}) \int C(y_{0_T}(\gamma)) f_{\Upsilon_{0_T}(|\nu_{0L}|^2)}(\gamma) d\gamma \\
&= (1-\varepsilon_{0L}) C\left(F_{|\nu_{0L}|^2}^{-1}(\varepsilon_{0L})\right) \\
&= (1-\varepsilon_{0L}) R_{0L}^{\varepsilon}.
\end{aligned}
\tag{25}
$$

We see that when only statistical turbulence-state knowledge is available to the data transmitter, the low-delay ergodic capacity is proportional to the ε-capacity. Most practical systems will require a low probability of outage, $\varepsilon \ll 1$. As a result, for most practical systems, the low-delay ergodic capacity with only statistical knowledge of the turbulence state at the transmitter is equal to the ε-capacity. The margin is a function of the fading distribution, specifically the distribution of $|\nu_{0L}|^2$, and we therefore do not include the calculation here.

Finally, we note that the optimal estimator and the single encoder-decoder estimator are the same when the data transmitter only has knowledge of the statistical distribution of the turbulence state,

$$
\begin{aligned}
R_{0L}^{\text{LD},s}(\varepsilon_{0L}) &= R_{0L}^{\text{LD}}(\varepsilon_{0L}) \\
y_{0_T}^s\left(\Upsilon_{0_T}\left(|\nu_{0L}|^2\right)\right) &= y_{0_T}\left(\Upsilon_{0_T}\left(|\nu_{0L}|^2\right)\right).
\end{aligned}
\tag{26}
$$

5.3 Shot-Noise Limited Turbulence-State Knowledge

We now provide an example calculation of the low-delay ergodic capacity for a specific system with coherent (heterodyne) detection at the data receiver, and signal shot-noise limited incoherent detection at the beacon receiver. For coherent detection at the data receiver, the low-delay ergodic capacity is

$$R_{0L}^{\text{LD}}(\varepsilon_{0L}) = \max_{y_{0_T}(\cdot):F_{|\nu_{0L}|^2|\Upsilon_{0_T}(|\nu_{0L}|^2)}(y_{0_T}(\gamma))<\varepsilon_{0L}\forall\gamma} (1-\varepsilon_{0L}) \int \log\left(1 + \frac{\alpha_{0L}P_{0_T}}{\sigma_{\text{osc}}^2} y_{0_T}(\gamma)\right) f_{\Upsilon_{0_T}(|\nu_{0L}|^2)}(\gamma) d\gamma, \tag{27}$$

where σ_{osc}^2 is the variance of the local-oscillator (LO) shot noise, which is Gaussian distributed in the strong-LO limit that is standard for heterodyne detection. To calculate the low-delay ergodic capacity, $R_{0L}^{\text{LD}}(\varepsilon_{0L})$, and the optimal estimator, $y_{0_T}(\cdot)$, we use Bayes' rule and the law of total probability to find the conditional distribution of $|\nu_{0L}|^2$ given $\Upsilon_{0_T}(|\nu_{0L}|^2)$, and the unconditional distribution of $\Upsilon_{0_T}(|\nu_{0L}|^2)$,

$$
\begin{aligned}
f_{|\nu_{0L}|^2}\left(\gamma|\,\Upsilon_{0_T}(|\nu_{0L}|^2) = y\right) &= \frac{f_{\Upsilon_{0_T}(|\nu_{0L}|^2)}\left(y|\,|\nu_{0L}|^2 = \gamma\right) f_{|\nu_{0L}|^2}(\gamma)}{\int f_{\Upsilon_{0_T}(|\nu_{0L}|^2)}\left(y|\,|\nu_{0L}|^2 = \gamma\right) f_{|\nu_{0L}|^2}(\gamma)\,d\gamma} \\
f_{\Upsilon_{0_T}(|\nu_{0L}|^2)}(y) &= \int f_{\Upsilon_{0_T}(|\nu_{0L}|^2)}\left(y|\,|\nu_{0L}|^2 = \gamma\right) f_{|\nu_{0L}|^2}(\gamma)\,d\gamma.
\end{aligned}
\tag{28}
$$

Because the channel state is observed at the data transmitter by an incoherent power meter, the observation of the channel state by the beacon receiver, $\Upsilon_{0_T}(|\nu_{0L}|^2)$, is obtained from a conditionally-Poisson random process with rate function $\mu_{0_R}(t)$. Moreover, because we assumed that the turbulence-state observation is signal shot-noise limited, i.e., $\alpha_{L0}P_{L_T} \gg \lambda^2 N_{0_\lambda} \Delta\lambda_0$, this rate function becomes

$$\mu_{0_R}(t) = \frac{\eta_0 \alpha_{L0}}{\hbar\omega_0} |\nu_{L0}(t)|^2 P_{L_T} \tag{29}$$

where we have taken the beacon transmitter to be unmodulated and operating at the peak-power limit P_{L_T} and assumed that α_{L0} is constant, as will be the case when adaptive optics are not employed. For a t_0-duration observation, where t_0 is less than the atmospheric coherence time, and a configuration exhibiting perfect ($|\nu_{0L}|^2 = |\nu_{L0}|^2$) reciprocity, the conditional distribution for $\Upsilon_{0_T}(|\nu_{0L}|^2)$ is then

$$\Pr\left(\Upsilon_{0_T}(|\nu_{0L}|^2) = k \,\middle|\, |\nu_{0L}|^2 = \gamma\right) = \frac{(\eta_0 \alpha_{L0} P_{L_T} \gamma t_0 \hbar \omega_0)^k}{k!} e^{-\eta_0 \alpha_{L0} P_{L_T} \gamma t_0 / \hbar \omega_0}. \tag{30}$$

By assuming some distribution for the turbulence-induced fading, such as gamma-gamma or lognormal, one can then numerically evaluate Eq. (28) and obtain the optimal estimator and the low-delay ergodic capacity. The single encoder-decoder estimator with its associated performance can also be found with numerical evaluation.

6. CONCLUSIONS

In the Part I paper, we showed that perfect reciprocity is exhibited within a wide range of conditions. For the common transmit-receive optical path, single-mode coupled system—as described in Section 2—reciprocity prevails regardless of the turbulence distribution along the propagation path, the size of the exit/entrance pupils $\mathcal{A}_0$ and $\mathcal{A}_L$, or the use of adaptive optics. In this Part II paper, we showed the *value* of reciprocity in terms of capacity, latency, and complexity for peak-power limited systems, although similar advantages accrue for average-power limited systems. Further, we showed techniques that exploit reciprocity by presenting an *optimal* architecture which maximizes capacity and a *suboptimal* architecture with greatly reduced implementation complexity compared to the optimal architecture. We calculated the performance of each architecture both based on theoretical systems. This paper does not address the design and performance of optical communication systems that uses reciprocity knowledge to achieve increased power transfer with an adaptive system—this topic was previously addressed by Shapiro.[1,3] The theoretical framework to evaluate the value of reciprocity presented in Section 3 is general enough to apply to systems that exhibit perfect reciprocity and systems that exhibit only partial reciprocity. For the examples, we only presented results for systems that exhibit perfect reciprocity. Future work should calculate the performance benefit for important situations that exhibit partial reciprocity—such as situations in which the point-ahead angle is large enough to cause partial reciprocity in a system that would experience perfect reciprocity with zero point-ahead angle. Additionally, this paper has focused on impact of reciprocity on the link layer, calculating performance for only a single link. Important future work includes a study of the impact of link layer sensing, including reciprocity, on heterogeneous network performance.

REFERENCES

[1] J. H. Shapiro, "Optimal power transfer through atmospheric turbulence using state knowledge," *IEEE Trans. Commun. Technol.* **19**, pp. 410–414, 1971.

[2] R. Lutomirski and H. Yura, "Propagation of a finite optical beam in an inhomogeneous medium," *Appl. Opt.* **10**, pp. 1652–1658, 1971.

[3] J. H. Shapiro, "Imaging and optical communication through atmospheric turbulence," in *Laser Beam Propagation in the atmosphere*, J. W. Strohbehn, Ed. Berlin, Springer-Verlag, 1978.

[4] J. H. Shapiro, "Reciprocity of the turbulent atmosphere," *J. Opt. Soc. Am.* **61**, pp. 492–495, 1971.

[5] J. H. Shapiro and A. Puryear, "Reciprocity-enhanced optical communication through atmospheric turbulence—Part I: Reciprocity proofs and far-field power transfer optimization," to be submitted to *Proc. SPIE*.

[6] J. A. Greco, "Design of the high-speed framing, FEC, and interleaving hardware used in a 5.4 km free-space optical communication experiment," *Proc. SPIE* **7464**, art. 746409, 2009.